

Upper ocean response to tropical storm Biparjoy in the Arabian Sea based on moored buoy observations

P K Kar*, K J Joseph, C A Prasad, R Janani, V M Mathew, M Kalyani & M A Muthiah

Ocean Observation Systems, National Institute of Ocean Technology, Chennai, Tamil Nadu – 600 100, India

*[E-mail: prabin.kar@gmail.com]

Received 21 March 2024; revised 11 May 2024

An Extremely Severe Cyclonic Storm (ESCS) ‘Biparjoy’ crossed very close to the moored buoys in the Arabian Sea (AS) during June 10-11, 2023 before its landfall on June 15 near Saurashtra and Kutch. The upper ocean response was examined, revealing significant changes in meteorological (wind, sea level pressure, and rainfall) and oceanic (waves, temperature, salinity profiles, and currents) parameters at AD06 and AD07, deployed by ocean observation systems group, National Institute of Ocean Technology (NIOT), Chennai. A spatial response study of Sea Surface Salinity (SSS) and Sea Surface Temperature (SST) was conducted to illustrate the pre- and post-cyclonic conditions.

On June 11, 2023, AD06 recorded Sea Level Pressure (SLP) drop to 965 hPa, 119.7 mm/day rainfall, and a maximum wind speed of 90 km/h (gustiness up to 153.7 km/h). At AD07, the wind peaked at 61.6 km/h on June 09, with SLP drop of 998.8 hPa on June 10, and 35.6 mm rainfall on June 11. SST dropped by ~ 4 °C at AD06 (June 12), and ~ 2 °C (June 10) at AD07. The Tropical Cyclone Heat Potential ~ 111 kJ/cm² and 135 kJ/cm² at AD06 and AD07, respectively favoured cyclone intensification. After June 11, the 26 °C isotherm (D26) shoaled significantly at AD06 (~ 24 m) with deepened mixed and isothermal layers, corresponding to enhanced cooling of SST at AD06 (~ 4 °C). Significant wave heights reached 8.9 m (AD06) and 7.29 m (AD07) with maximum wave heights of 14.6 m and 11.46 m, respectively, on 12th and 10th June. The spatial distribution of SST and SSS during the post-cyclone phase is marked by notable cooling (~ 27 °C) and an increase in salinity (~ 36 ppt) in the upper layers of the AS.

[**Keywords:** Arabian Sea, Cyclonic storm, Met-ocean parameters, Moored buoy, Ocean response]

Introduction

Frequent extreme events such as cyclonic storms are very common in this climate change era due to the dynamic changes in weather and climate. Ocean observations support weather and climate monitoring, aiding resource and ecosystem management as well as disaster mitigation which significantly impact human life¹. The intensity of severe cyclonic storms in the North Indian Ocean (NIO) region had an increasing trend in the last four decades². National Institute of Ocean Technology (NIOT) maintains a network of moored buoys fitted with automated sensors for the real-time monitoring of the marine environment since its inception in 1997.

The occurrence of Tropical Cyclones (TCs) in the NIO are maximum during October – December (post-monsoon) followed by the secondary peak during April – June (pre-monsoon)³. The disturbances developed during pre-monsoon season in NIO have a higher probability of intensifying as Severe Cyclonic Storms (SCS) compared to those during post-monsoon⁴. The primary cause of the recent rise in pre-monsoon

tropical storm intensity in the Arabian Sea (AS) is related to the decrease in the vertical wind shear in the troposphere⁵. In recent decades, the frequency and duration of TCs over the AS increased compared to those in the Bay of Bengal (BoB)⁶. Especially, between 1998 and 2019, about 10 storms in the northern Arabian Sea intensified into severe cyclones⁷. Similarly, during 1965 – 2022, 66 cyclonic storms with maximum sustained wind speed exceeding 62 kmph developed over the AS^(ref. 8). Out of these, 8 crossed the Gujarat coast. The Extremely Severe Cyclonic Storm (ESCS) Biparjoy recorded the second largest life span of 13 days and three hours over the NIO after the cyclone in 1977, with a life span of 14 days and six hours⁸. However, based on data from 1990 to 2013, the ESCS category's average life span over the AS during monsoon season is six days and three hours⁸.

Numerous studies associated with cyclone-induced impacts in the AS have been extensively carried out by several authors, including Terry & Gienko⁹; Murakami *et al.*¹⁰; Hussain *et al.*¹¹; and Evan *et al.*¹².

More specifically, importance of buoy data in deciphering the upper ocean and sub-surface variability during cyclone Roanu¹³, Phailin¹⁴, Viyaru¹⁵, Amphan¹⁶, and Thane¹⁷ has been well documented. Intense cyclones have severe impacts on coastal areas, making it crucial to monitor their intensification and track them while they are over the ocean. Moored buoy platforms at sea play a vital role in observing and predicting ocean conditions, which helps forecast cyclone intensity. In a more recent study by Maneesha *et al.*¹⁸ used both model and *in-situ* data for the cyclone Biparjoy to understand the causes for its intensification in the AS. Their results showed the importance of increased stratification under the inflow of warm and high saline waters from the north and subsequent increase in the heat content of the upper ocean. In the present study, though only one cyclone is examined, study used *in-situ* water column data on temperature and salinity from moored buoys along with data on met-ocean parameters from the buoy to quantify the cyclone-induced changes.

Materials and Methods

The OMNI (Ocean Moored Buoy Network for Northern Indian Ocean) buoys were deployed by NIOT to collect the oceanographic and meteorological parameters along with subsurface data on waves, currents, temperature and salinity. The study used the *in situ* parameters, such as wind speed, wind direction, Sea Level Pressure (SLP), and rainfall at three-meter height (wind speed converted to 10 m) of AD06 (18°19'18.58" N & 67°20'03.06" E) and AD07 (14°55'29" N & 68°58'06" E) and oceanic parameters such as wave, sea surface and subsurface temperature, current profiles were obtained from 1st June 2023 to 16th June 2023 at an interval of 3 h by the moored buoys to depict the dynamic changes under the influence of ESCS Biparjoy. Detailed information on both the moored buoys are presented in Table 1. The cumulative rainfall data obtained from both the buoys were further converted to daily rainfall. Using the temperature profile data,

Isothermal Layer Depth (ILD) was calculated by determining the depth at which the temperature at 10 m exceeded by 0.5 °C. Though data at 1 m, 5 m, and 10 m depths are available from the moored buoy, the data at 10 m has been used in the present study, as uninterrupted data is available at this depth for the period of study. Using the temperature and salinity profiles density has been calculated, which was further used for the determination the MLD. The MLD was calculated as the depth at which a 0.5 °C rise in temperature is equivalent to a density increase in relation to the 10 m reference level¹⁹. All time-series data have been smoothed with a 24 h running mean. The Tropical Cyclone Heat Potential (TCHP), which is an important parameter for the cyclogenesis has been calculated using:

$$TCHP = \rho C_p \int_0^{D26} [T(z) - 26] dz$$

Where, ρ is the average density of seawater at the surface (assumed constant), C_p is the specific heat capacity of seawater at constant pressure p , T is the temperature (°C), and $D26$ is the depth of the 26 °C isotherm²⁰. The TCHP is in kJ/cm². Further, high-resolution SST (1 km) from the Group of High Resolution SST (GHRSSST)²¹ and surface salinity (SSS) (25 km) was obtained from the NASA Soil Moisture Active Passive (SMAP) satellite observatory¹⁶. The SMAP L3 daily running mean SSS and SST data, captured during the cyclone as well as one week before and after, is presented to quantify the impact on SSS and SST. Changes in SST/SSS following the passage of cyclone Biparjoy were computed by subtracting SST/SSS data before one week of its formation and after one week of its landfall.

Cyclone Biparjoy

ESCS Biparjoy classified as a category-3 storm on the Saffir-Simpson wind scale²², crossed very close to AD06 and AD07 moored buoy location in the AS on 10th – 12th of June, 2023 and had a landfall on 15th June 2023 near Saurashtra and Kutch adjoining Pakistan coasts between Mandvi and Karachi⁸

Table 1 — Location of moored buoys AD06 and AD07 used for the present study in AS during the transit of Biparjoy cyclone

	AD06	AD07
Position	Left side of the track	Right side of the track
Coordinates	18°19'18.58" N & 67°20'03.06" E	14°55'29" N & 68°58'06" E
Minimum distance of buoy from track	11.4 Nautical miles	107.1 Nautical miles
Date when the cyclone is closest to the buoy location	11.06.2023 - 3GMT to 9GMT	09.06.2023 - 12 GMT to 15GMT
Depth of the mooring	3485 m	4008 m

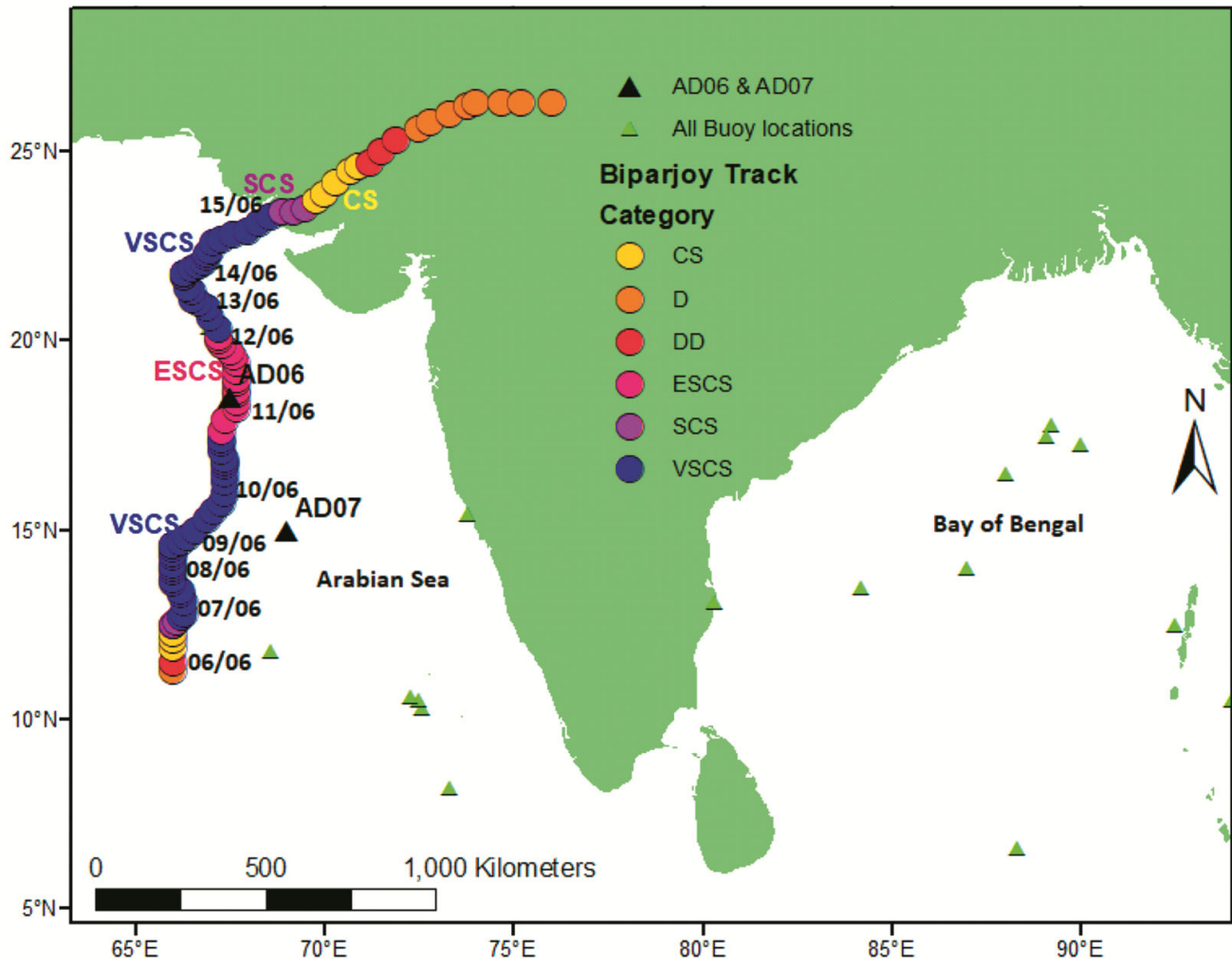


Fig. 1 — Study area showing the track of the cyclone Biparjoy. Locations of the data buoy AD06 and AD07 are shown as filled triangles

(Fig. 1). It crossed very close to Jakhau port of Gujarat between 22:30 and 23:30 hrs IST on 15th June. It was the first cyclonic storm over the AS in 2023 with a progressive translation speed of 2.33 m/s, which continued until 16th June, 2023^(ref. 18). The moored buoys AD06 and AD07 provided continuous surface and subsurface data during the life cycle of Biparjoy.

Results

In situ observations and upper ocean response

Figure 2 depicts the met-ocean parameters such as significant wave height (m), highest wave height (m), SST (at 1 m depth), rainfall (mm), SLP and wind speed.

The immediate response of Biparjoy was observed on 11th June 2023 as a low-pressure of 965 hPa, a maximum rainfall of 119.7 mm/day, and a maximum

wind speed of up to 25 m/s with gusts up to 44.6 m/s at AD06 buoy (Fig. 2). Similarly, AD07 moored buoy also recorded a maximum wind speed of 17.2 m/s on 9th June with SLP of 998.8 hPa on 10th June and 35.6 mm of maximum rainfall on 11th June 2023. The initial increase of wind speed and drop of SLP started on 9th June which further reached its extreme on 11th at AD06 and on 9th at AD07. The maximum drop ~ 4 °C on 12th June and ~ 2 °C on 10th June in SST was observed at AD06 and AD07, respectively. After the cyclone track crossed the buoy locations, the corresponding SSTs lowered substantially due to the wind mixing of the oceans¹⁶. Both the moored buoy data indicated the response of the cyclone as the drop of SLP is associated with rapid cooling of SST. The response observed at AD07 is comparatively less than that of AD06 since it is 107.1 nm away from the cyclone track, whereas AD06 was at a distance of

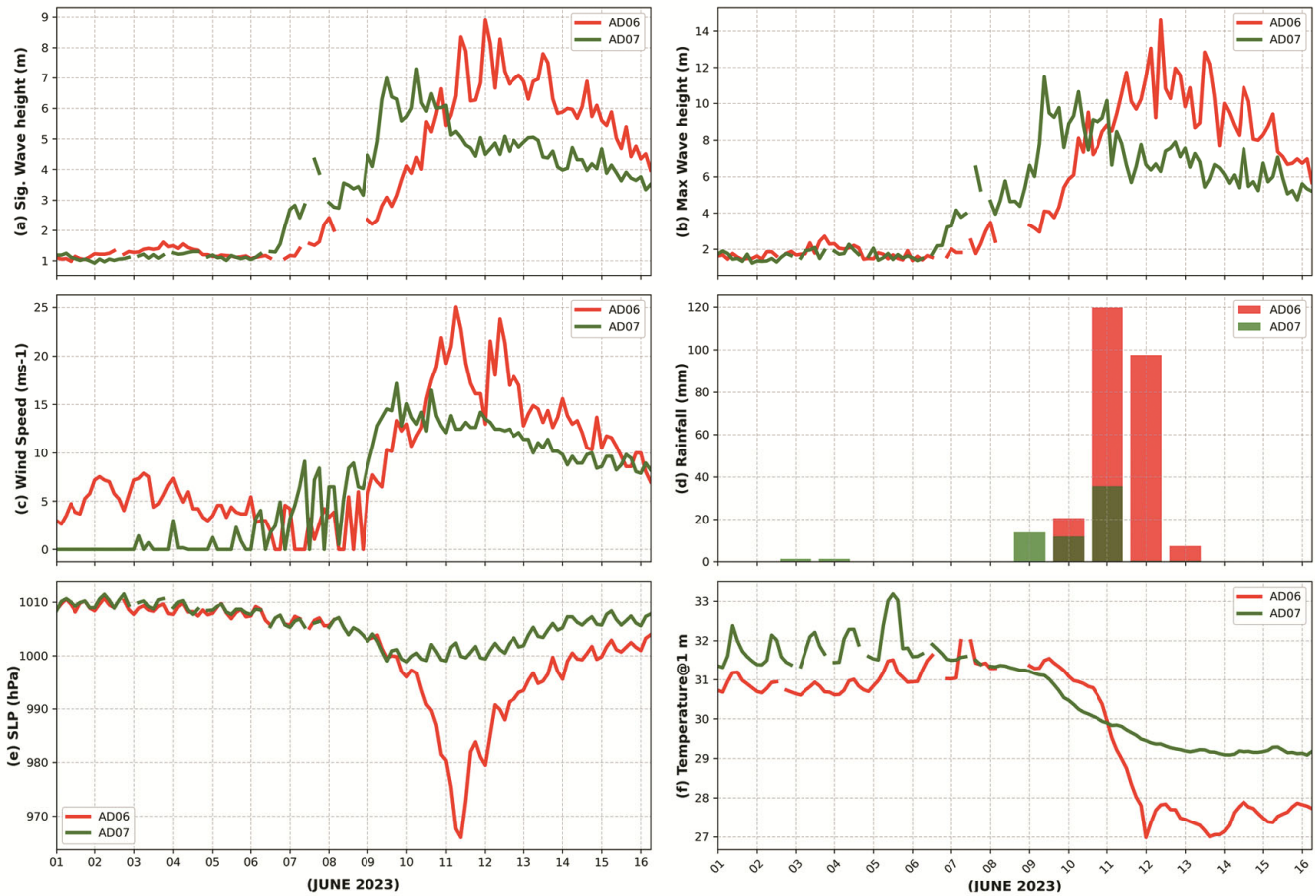


Fig. 2 — Temporal evolution of Temperature at 1 m, significant wave height (m), maximum wave height (m), rainfall (mm), sea level pressure (hPa), and wind speed (m/s) at AD06 (redline) and AD07 (green line) during 1st – 16th June, 2023

only 11.4 nm (Table 1). During the passage of the ESCS Biparjoy at AD06, the maximum wave height was 14.6 m, while it was 11.5 m at AD07. The buoy AD06 and AD07 also recorded a significant wave height of 8.9 m (12th June 2023) and 7.29 m, on 10th June 2023, indicating the severity of the sea state during the cyclone passage.

Wind, current, and wave parameters have a significant influence on the inducement of TCs. Figure 3 depicts the wind, wave and current roses for AD06 and AD07 locations before, during and after the passage of the cyclone. Deep ocean currents are produced by local wind and incident waves and play a vital role in changing the mixed layer pattern²³. It is observed that in both AD06 and AD07, before the event, the current speeds were overall lower, while the current direction was not uniform. A significant portion of time falls into the calm category (75.6 % calm) in both AD06 and AD07. However, during the event, it dropped sharply (59.52 % calm in both AD06 and AD07) while it was moving northward direction

predominantly (Fig. 3). There’s a significant increase in current speed, particularly in AD06. This suggests the event caused stronger currents in specific directions, with a dramatic reduction in calm conditions. After the passage of the cyclone, the calm period increases again (87.50 % calm in AD07), indicating a return to calmer conditions.

Before the event, wave heights were relatively low, approaching randomly from all directions. However, during the event, wave heights significantly increased (> 7.6 m) which shows the severity of the sea state at AD06, while AD07 also showed increased wave activity but at slightly lower heights. Post-cyclone wave heights decrease again, though not as dramatically as in the current speed. The wind speeds were relatively lower magnitude before the event, predominantly blowing from the southwest for both the locations with high calm percentages (96.4 % in AD06 and AD07), which further increases significantly during the event. Particularly at AD06, the strong wind was above 19.6 m/s during the

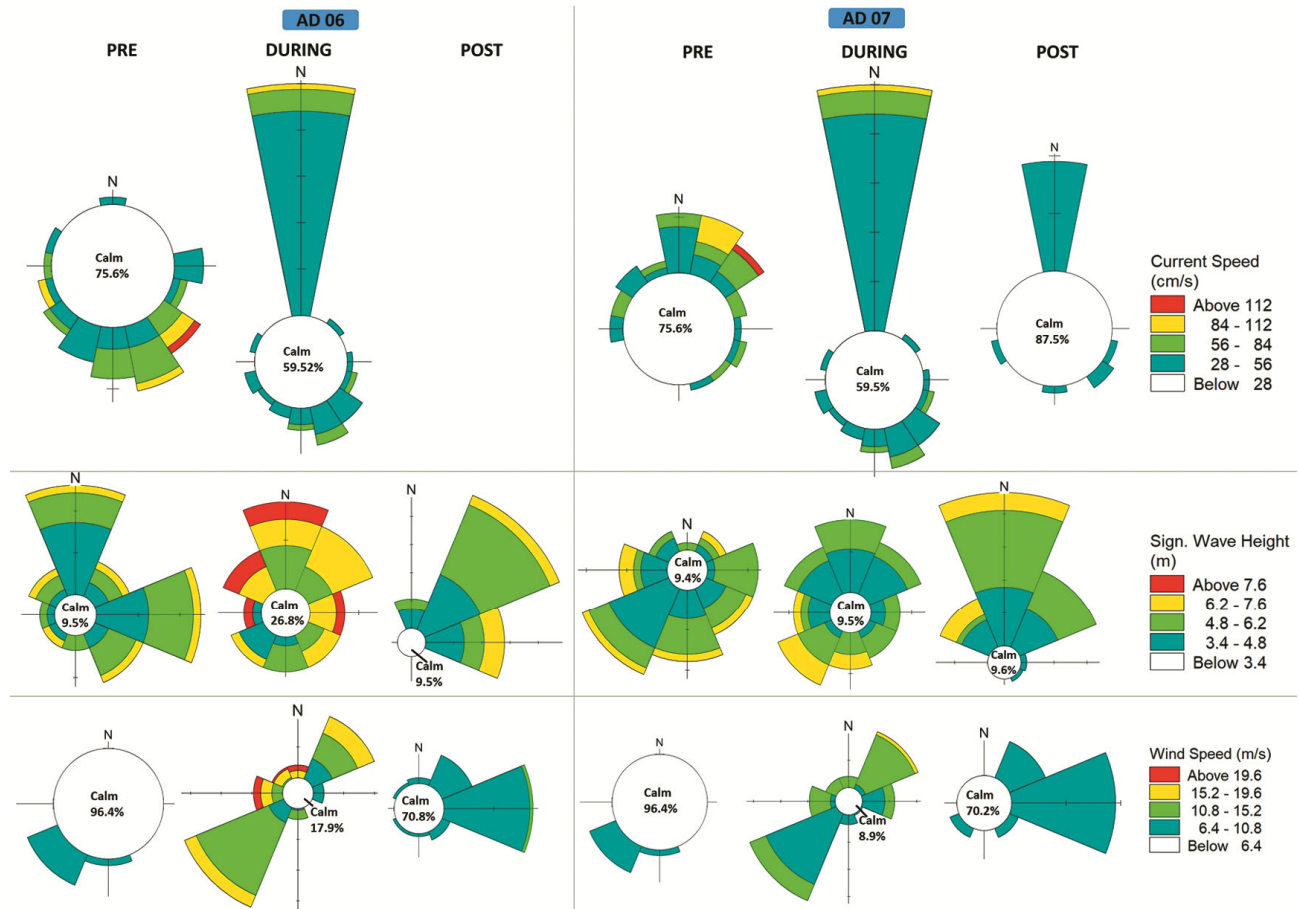


Fig. 3 — Wind (m/s), wave (m), and current (cm/s) before, during and after the passage of the TC Biparjoy (01 – 21 June 2023) near moored buoy location

passage of the cyclone. The calm condition decreases to 17.9 % in AD06 and 8.9 % in AD07). After the cyclone, wind speed reduced significantly and calm percentages recovered (70.8 % in AD06 and 70.2 % in AD07).

Spatial response of SST and SSS

TCs have significant physical impacts on the upper ocean, which manifest as SST cooling and SSS increase. Figure 4 shows the spatial distribution of SST and SSS during the cyclonic period (6 – 15 June) (Fig. 4b & f); 7-day average SST during the pre-cyclonic period (one week before) (Fig. 4a & e); and post-cyclonic periods (one week after) (Fig. 4c & g) of the ESCS Biparjoy. Figure 3(d & h) shows the difference in SST and SSS, respectively, obtained by subtracting the data after one week from the data before one week²¹.

The pre-cyclone phase was warmer than the post-cyclone period (Fig. 4a). In the difference plots

(Fig. 4d), the post-cyclone phase cooled by more than 3 °C. The whole north and central AS SST cooled generally after the passage of the cyclone. During the passage of the cyclone, the SST was warmer near AD07 than at the AD06 location (Fig. 4b). But areas further offshore experienced a noticeable cooling effect, likely due to increased mixing from the cyclone's wind-induced turbulence. After the passage of the cyclone, this cooling effect is most prominent around AD06 and AD07 (Fig. 4c), indicating the cyclone facilitated mixed cooling of subsurface water with warmer surface water, leading to a drop in SST. These cooling patterns are centred around the cyclone's track, confirming the cooling impact of cyclonic activity due to upwelling.

The SSS plots (Fig. 4e – h) show the TC-induced increase in salinity after the passage of the cyclone (Fig. 4g) due to the Ekman suction and wind mixing²⁴. However, during the cyclone (Fig. 4f), there

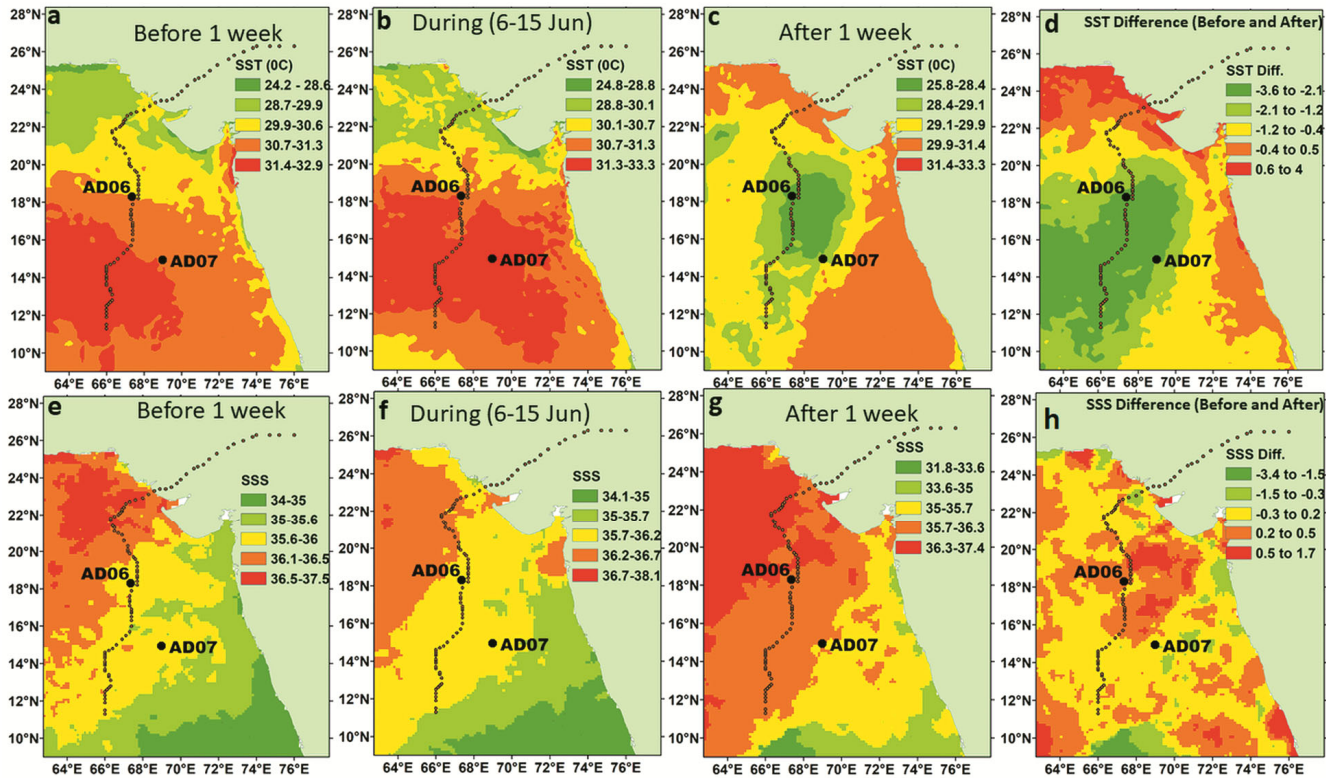


Fig. 4 — The SST (°C) based on GHRSST in the Arabian Sea during: (a) pre-Biparjoy (1 week before), (b) during Biparjoy (6 – 15 June 2023), (c) post-Biparjoy (1 week after), and (d) changes in SST following the passage of cyclone Biparjoy. The SSS based on SMAP during: (e) pre-Biparjoy (1 week before), (f) during Biparjoy (6 – 15 June 2023), (g) post-Biparjoy (1 week after), and (d) changes in SSS following the passage of cyclone Biparjoy

was a noticeable shift in SSS, especially in areas impacted by the cyclone. The cyclone likely caused a mixing of surface and deeper waters, altering the salinity distribution. The magnitude of the positive SSS response is comparable with the buoy real-time data, which reveals the reliability of the SMAP data on TC-induced SSS response during the storm passage.

Temperature profile, MLD/ILD before and after ESCS Biparjoy

The immediate response of ESCS Biparjoy and detailed analysis of the temperature profile corresponding to Isothermal Layer Depth (ILD) and Mixed Layer Depth (MLD) is depicted in Figure 5 for AD06 and in Figure 6 for AD07 (MLD and ILD - Top panel, and temperature profile - bottom panel). Significant reduction in temperature was noted in the upper ocean at both locations during the passage of the ESCS Biparjoy.

The temperature profile in Figure 5 shows the warmer SST in pre-monsoon before the cyclone passage in the AS at AD06. The MLD was also in

the range of 12.3 – 33.6 m and ILD of 17 – 40 m. As the cyclone got closer to the moored buoy, a significant deepening in MLD and ILD was noticed due to cyclone-induced wind forcing. In particular, starting on June 9th, the MLD and ILD were repeatedly deepening (points 1 – 4) in response to the intense cyclone, with points 3 and 4 having maximum cyclone impact. After the passage of the cyclone on 11th June 2023, a significant reduction of temperature and thinning of the mixed layer and isotherm layer were observed for 6 h (15 – 21 GMT of 11th June), but deepened once again afterwards due to cyclone induced wind-mixing. The deeper layer of temperature at AD06 has shown significant semidiurnal fluctuation following the cyclone (Fig. 5). It appears that the vertical gradient in the temperature profile during post-cyclone scenario resulted in the deepening of MLD/ILD and cooling SST.

Figure 6 depicts the time-varying temperature up to 500 m depth along with MLD and ILD at AD07. Results clearly distinguish the ocean response before

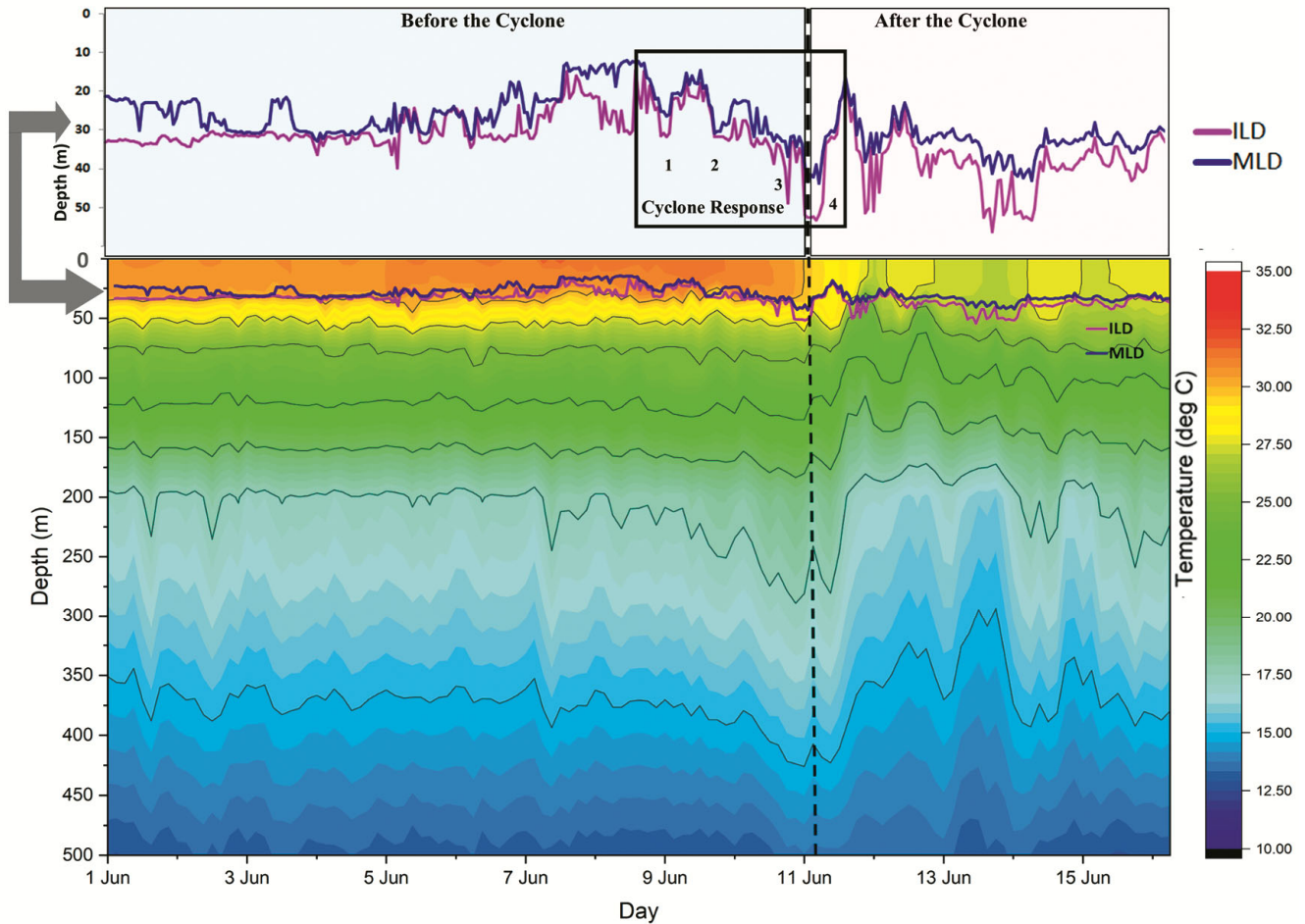


Fig. 5 — Time series of the upper ocean temperature up to 500 m (bottom panel) and with ILD (pink line) and MLD (blue line) (top panel) at AD06 during 01 – 16 June, 2023. The black rectangle in the top panel represent the duration of cyclone. Vertical dashed black line represents the cyclone passage at buoy location

and after the cyclone. The temperature in the top 30 m was decreased by ~ 1.5 °C. Simultaneously, the ILD deepened (> 50 m) and continued till the landfall (Fig. 6, top panel). The temperature profile shows a clear stratification in the ocean, with warmer temperatures near the surface (above 50 m) and a gradient cooling effect in the deeper layer (Fig. 6, bottom panel). Post-cyclone ocean response indicates the warm surface layer cools down slightly, and the mixing effect penetrates deeper into the ocean.

Role of upper ocean parameters in intensifying cyclones

Tropical cyclones and their intensification are mainly influenced by TCHP and upper ocean stratification, which have greater importance in the intensification of tropical cyclones²⁵. TCHP rather than SST has a major influence on the intensification of TCs²⁶. It is, therefore, crucial to comprehend the

function of the upper ocean in terms of both TC intensification and maximum intensity.

Cyclone-induced rapid change in TCHP was observed at AD06, while it was moderate at AD07 as the buoy location was far away from the cyclone track (Table 1). The maximum TCHP was ~ 135 kJ/cm² at AD07 and 111.7 kJ/cm² at AD06, which is favourable for the intensification of the cyclone. A decrease of ~ 70 kJ/cm² was observed after the eye of the cyclone crossed at AD06 (Fig. 7). D26 at AD06 location fluctuated significantly, showing rapid changes in depth, reaching up to ~ 24 m during the cyclone event around June 11th suggesting that upwelling due to intense mixing dominated. The storm-driven wind drives upwelling of cooler waters, causing 26 °C isotherm to become shallower. AD07, exhibited more resistance to these changes, maintaining a deeper and more stable 26 °C isotherm even in the presence of a cyclone.

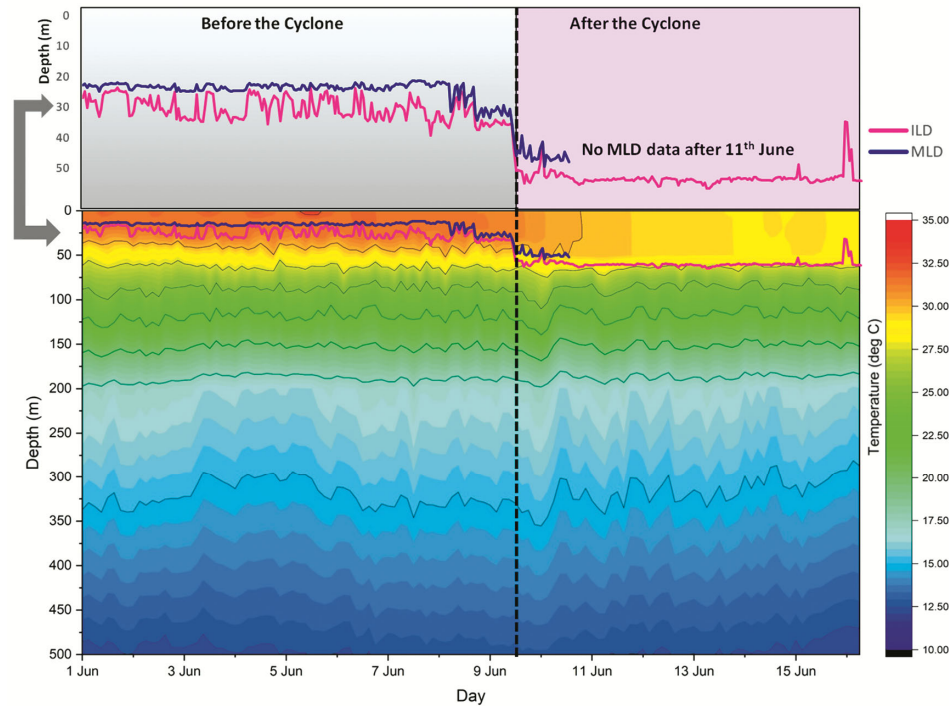


Fig. 6 — Time series of the upper ocean temperature up to 500 m (bottom panel) and with ILD (pink line) and MLD (blue line) (top panel) at AD07 during 01 – 16 June, 2023. Vertical dashed black line represents the cyclone passage at buoy location

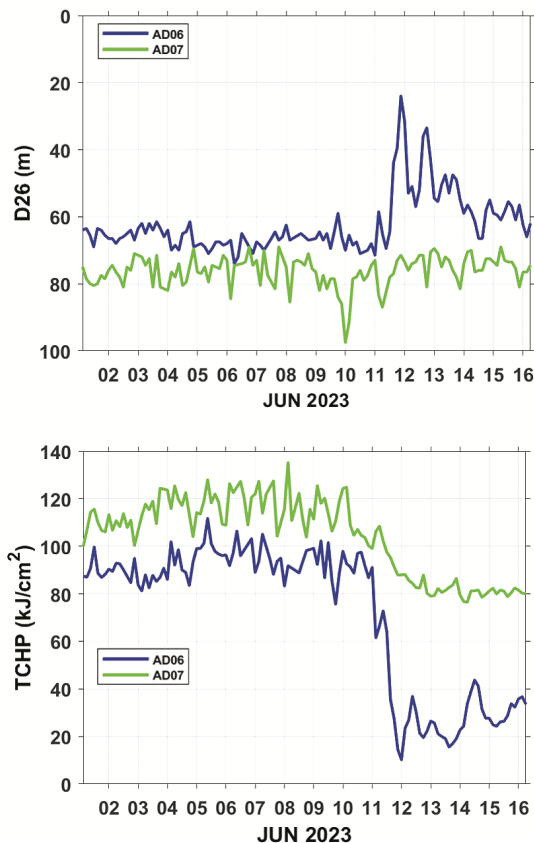


Fig. 7 — Depth of 26 °C isotherm & estimated TCHP using data from AD06 and AD07 during Biparjoy

Discussion and Conclusion

Intense cyclones have a profound impact on coastal regions, causing significant damage in various ways^{27,28}. Therefore, it is vital to monitor their intensification and track their movement while they are over the ocean. Comprehensive data on met-ocean parameters play a crucial role in understanding cyclones, monsoons and climatic changes^{14,29}. Cyclone Biparjoy, which made landfall on the Gujarat coast in June 2023, was notable for several reasons, including its extended duration and socio-economic impacts. This cyclone set a record for the longest duration in the history of AS, maintaining its strength for 192 h, possibly due to the unusually warm waters (> 31 °C) of the AS (Fig. 4a – c). Significant alterations in the surface meteorological and oceanic parameters were noted during the passage of the intense ESCS Biparjoy. Cyclone-induced changes in met-ocean parameters were most pronounced as the track got closer to the buoys AD06 and AD07. ESCS Biparjoy in 2023 was incredibly slow, at less than 8 km/h, making a landing in Gujarat, India, on June 15th, 2023. With 13 days and three hours duration from depression (formative stage) to depression (dissipative stage), Biparjoy was one of the long-lasting cyclones having a track length of 2525 km in the NIO⁸. The persistence of Biparjoy over a longer

period in parts might have sustained due to the warmer SST ($> 31\text{ }^{\circ}\text{C}$) and the high TCHP during the cyclone period. The advection of warm and salty waters of the AS was strongly impacted by the upper ocean heat content⁷. This, in turn, appears to have created a favourable environment for the formation and rapid intensification of cyclones, as in the case of Biparjoy. The drop in SST associated with the cyclone seen at AD06 is the result of Ekman dynamics and associated mixing during the passage of Biparjoy. This study has highlighted the utility of the in situ measured data sets in monitoring cyclones in real-time by the surface meteorological parameters and subsurface ocean parameters by the data buoys with sensors attached at different depths. The assimilation of moored buoy data into the operational models would further facilitate better forecasting of cyclonic weather systems.

Acknowledgements

The authors are grateful to the Director, NIOT and Ministry of Earth Sciences, Govt. of India, for providing the essential facilities. The authors are also thankful to the organizers of the World Ocean Science Congress-2024 for recommending the manuscript to be included in the IJMS special issue. Authors acknowledge the support extended by the OOS team at NIOT in the maintenance of the moored buoy network in the Indian Seas. The authors extend their sincere gratitude to Dr. S. Prasanna Kumar, Former Chief Scientist, NIO, Goa; Dr. Subhasis Pradhan, NCCR; and all the reviewers for their insightful and constructive feedback, which significantly contributed to improving the quality of the manuscript.

Conflict of Interest

The authors declare that they have no known competing financial interests or personal relationships that could have appeared to influence the work reported in this paper.

Ethical Statement

All of the authors have read and approved the manuscript and it has neither been published previously nor is it under consideration by any other peer-reviewed journal. All authors have been personally and actively involved in substantive work leading to the manuscript and will hold themselves jointly and individually responsible for its content.

Author Contributions

PKK: Planning of the work, manuscript preparation, and writing - original draft; KJJ: Conceptualization, supervision, planning of the work, and review & editing; CAP, RJ & VMM: Data compilation, formal analysis, mapping, interpretation, and manuscript preparation; and MK & MAM: Given valuable input and critical feedback to strengthen the manuscript standard.

References

- Venkatesan R, Tandon A, Sengupta D & Navaneeth K N, Recent trends in ocean observations, In: *Observing the Oceans in Real Time*, edited by Venkatesan R, Tandon A, D'Asaro E & Atmanand M A, (Springer, Cham), 2018, pp. 3-13. https://doi.org/10.1007/978-3-319-66493-4_1
- Albert J, Krishnan A, Bhaskaran P K & Singh K S, Role and influence of key atmospheric parameters in large-scale environmental flow associated with tropical cyclogenesis and ENSO in the North Indian Ocean basin, *Clim Dyn*, 58 (2022) 17-34. <https://doi.org/10.1007/s00382-021-05885-8>
- Mahala B K, Nayak B K & Mohanty P K, Impacts of ENSO and IOD on tropical cyclone activity in the Bay of Bengal, *Nat Hazards*, 75 (2015) 1105-1125. <https://doi.org/10.1007/s11069-014-1360-8>
- Yanase W, Satoh M, Taniguchi H & Fujinami H, Seasonal and intraseasonal modulation of tropical cyclogenesis environment over the Bay of Bengal during the extended summer monsoon, *J Clim*, 25 (2012) 2914-2930. <https://doi.org/10.1175/JCLI-D-11-00208.1>
- Wang B, Xu S & Wu L, Intensified Arabian Sea tropical storms, *Nature*, 489 (2012) (7416) E1-E2. <https://doi.org/10.1038/nature11470>
- Fan X T, Li Y, Lyu A M & Liu L S, Statistical and comparative analysis of tropical cyclone activity over the Arabian Sea and Bay of Bengal (1977-2018), *J Trop Meteorol*, 26 (3) (2020) 441-452. <https://doi.org/10.46267/j.1006-8775.2020.038>
- Maneesha K, Brahmananda R V, Patnaik K V K R K & Franchito S H, The Intrusion of Spicy Water Favours the Intensification of Arabian Sea Cyclones, *Atmos-Ocean*, 61 (2) (2023) 84-93. <https://doi.org/10.1080/07055900.2022.2118106>
- IMD, *Extremely Severe Cyclonic Storm "BIPARJOY" over the Arabian Sea, (6th-19th June, 2023): A Report*, India Meteorological Department, 2023. Accessed online at: <https://rsmcnewdelhi.imd.gov.in>
- Terry J P & Gienko G, Quantitative observations on tropical cyclone tracks in the Arabian Sea, *Theor Appl Climatol*, 135 (2019) 1413-1421. <https://doi.org/10.1007/s00704-018-2445-1>
- Murakami H, Vecchi G A & Underwood S, Increasing frequency of extremely severe cyclonic storms over the Arabian Sea, *Nat Clim Change*, 7 (12) (2017) 885-889. <https://doi.org/10.1038/s41558-017-0008-6>
- Hussain M A, Abbas S & Ansari M R K, Persistency analysis of cyclone history in Arabian sea, *Nucleus*, 48 (4) (2011) 273-277. <https://doi.org/10.71330/thenucleus.2011.820>

- 12 Evan A T, Kossin J P, Chung C E & Ramanathan V, Arabian Sea tropical cyclones intensified by emissions of black carbon and other aerosols, *Nature*, 479 (7371) (2011) 94-97. <https://doi.org/10.1038/nature10552>
- 13 Mandal S, Sil S, Shee A & Venkatesan R, Upper ocean and subsurface variability in the Bay of Bengal during cyclone ROANU: A synergistic view using in situ and satellite observations, *Pure Appl Geophys*, 175 (2018) 4605-4624. <https://doi.org/10.1007/s00024-018-1932-8>
- 14 Venkatesan R, Mathew S, Vimala J, Latha G, Muthiah M A, *et al.*, Signatures of very severe cyclonic storm Phailin in met-ocean parameters observed by moored buoy network in the Bay of Bengal, *Curr Sci*, 107 (4) (2014) 589-595. <https://www.jstor.org/stable/24103530>
- 15 Venkatesan R, Joseph K J, Prasad C A, Muthiah M A, Ramasundaram S, *et al.*, Differential upper ocean response depicted in moored buoy observations during the pre-monsoon cyclone Viyaru, *Curr Sci*, 118 (11) (2020) 1760-1767. <https://www.jstor.org/stable/27138821>
- 16 Bhowmick S A, Agarwal N, Sharma R, Sundar R, Venkatesan R, *et al.*, Cyclone Amphan: oceanic conditions pre- and post-cyclone using *in situ* and satellite observations, *Curr Sci*, 119 (9) (2020) 1510-1516. <https://www.jstor.org/stable/27139056>
- 17 Mathew S, Natesan U, Latha G, Venkatesan R, Rao R R, *et al.*, Observed warming of sea surface temperature in response to tropical cyclone Thane in the Bay of Bengal, *Curr Sci*, 114 (7) (2018) 1407-1413. <https://www.jstor.org/stable/26495495>
- 18 Maneesha K, Effect of "spiciness" on the intensification of cyclones over Arabian Sea-a case study on Biparjoy, *Clim Dyn*, 62 (5) (2024) 3955-3963. <https://doi.org/10.1007/s00382-024-07109-1>
- 19 Price J F, Weller R A, Pinkel R, Diurnal cycling: observations and models of the upper ocean response to diurnal heating, cooling, and wind mixing, *J Geophys Res Ocean*, 91 (1986) 8411-8427. <https://doi.org/10.1029/JC091iC07p08411>
- 20 Leipper D F & Volgenau D, Hurricane heat potential of the Gulf of Mexico, *J Phys Oceanogr*, 2 (3) (1972) 218-224. [https://doi.org/10.1175/1520-0485\(1972\)002%3C0218:HHPOTG%3E2.0.CO;2](https://doi.org/10.1175/1520-0485(1972)002%3C0218:HHPOTG%3E2.0.CO;2)
- 21 Navaneeth K N, Martin M V, Joseph K J & Venkatesan R, Contrasting the upper ocean response to two intense cyclones in the Bay of Bengal, *Deep-Sea Res I: Oceanogr Res Pap*, 147 (2019) 65-78. <https://doi.org/10.1016/j.dsr.2019.03.010>
- 22 Parmar S P, A Comprehensive Study of Biparjoy Cyclone Disaster Management in Gujarat: A Case Study, *Eng OA*, 2 (3) (2024) 01-17.
- 23 Shankar D, Remya R, Vinayachandran P N, Chatterjee A & Behera A, Inhibition of mixed-layer deepening during winter in the northeastern Arabian Sea by the West India Coastal Current, *Clim Dyn*, 47 (3) (2016) 1049-1072. <https://doi.org/10.1007/s00382-015-2888-3>
- 24 Sun J, Vecchi G & Soden B, Sea surface salinity response to tropical cyclones based on satellite observations, *Remote Sens*, 13 (3) (2021) 1-25. <https://doi.org/10.3390/rs13030420>
- 25 Maneesha K, Sadhuram Y & Prasad K V S R, Role of upper ocean parameters in the genesis, intensification and tracks of cyclones over the Bay of Bengal, *J Oper Oceanogr*, 8 (2) (2015) 133-146. <https://doi.org/10.1080/1755876X.2015.1087185>
- 26 Jangir B, Swain D & Bhaskar T U, Relation between tropical cyclone heat potential and cyclone intensity in the North Indian Ocean, In: *Remote sensing and modeling of the atmosphere, oceans, and interactions VI*, Vol 9882, SPIE Asia-Pacific Remote Sensing, 2016, New Delhi, India, 2016, pp. 359-365. <https://doi.org/10.1117/12.2228033>
- 27 Kar P K, Mohanty P K, Pradhan S, Behera B, Padhi S K, *et al.*, Shoreline change along Odisha Coast using statistical and geo-spatial techniques, *J Earth Syst Sci*, 130 (209) (2021) 1-20. <https://doi.org/10.1007/s12040-021-01703-1>
- 28 Mohanty P K, Kar P K & Behera B, Impact of very severe cyclonic storm Phailin on shoreline change along South Odisha Coast, *Nat Hazards*, 102 (2020) 633-644. <https://doi.org/10.1007/s11069-019-03610-7>
- 29 Woodworth P L, Have there been large recent sea level changes in the Maldiv Islands? *Glob Planet Change*, 49 (2005) 1-18. <https://doi.org/10.1016/j.gloplacha.2005.04.001>